η and η′ mesons in the Dyson-Schwinger approach at finite temperature

Horvatić, Davor; Klabučar, Dubravko; Radzhabov, A. E.

Source / Izvornik: **Physical Review D - Particles, Fields, Gravitation and Cosmology, 2007, 76**

Journal article, Published version
Rad u časopisu, Objavljena verzija rada (izdavačev PDF)

https://doi.org/10.1103/PhysRevD.76.096009

Permanent link / Trajna poveznica: https://urn.nsk.hr/urn:nbn:hr:217:480454

η and η' mesons in the Dyson-Schwinger approach at finite temperature

D. Horvatić,[1,*] D. Klabučar,[1,2,†,‡] and A. E. Radzhabov[3,§]

[1]*Physics Department, Faculty of Science, University of Zagreb, Bijenička c. 32, Zagreb 10000, Croatia*
[2]*Senior Associate of International Centre for Theoretical Physics, Trieste, Italy*
[3]*Bogoliubov Laboratory of Theoretical Physics, Joint Institute for Nuclear Research, 141980 Dubna, Russia*

(Received 10 August 2007; published 29 November 2007)

We study the temperature dependence of the pseudoscalar meson properties in a relativistic bound-state approach exhibiting the chiral behavior mandated by QCD. Concretely, we adopt the Dyson-Schwinger approach with a rank-2 separable model interaction. After extending the model to the strange sector and fixing its parameters at zero temperature, $T = 0$, we study the T dependence of the masses and decay constants of all ground-state mesons in the pseudoscalar nonet. Of chief interest are η and η'. The influence of the QCD axial anomaly on them is successfully obtained through the Witten-Veneziano relation at $T = 0$. The same approach is then extended to $T > 0$, using lattice QCD results for the topological susceptibility. The most conspicuous finding is an increase of the η' mass around the chiral restoration temperature T_{Ch}, which would suggest a suppression of η' production in relativistic heavy-ion collisions. The increase of the η' mass may also indicate that the extension of the Witten-Veneziano relation to finite temperatures becomes unreliable around and above T_{Ch}. Possibilities of an improved treatment are discussed.

DOI: 10.1103/PhysRevD.76.096009 PACS numbers: 11.10.St, 11.10.Wx, 12.38.−t, 14.40.Aq

I. INTRODUCTION AND PRELIMINARIES

The experiments at Relativistic Heavy Ion Collider (RHIC) advanced the empirical knowledge about relativistic hot QCD matter dramatically [1,2], but its properties are so intricate that the understanding of the state of matter that has been formed is still to be developed [2]. Prior to its observation at RHIC, the hot QCD matter, usually called quark-gluon plasma (QGP), was pictured as a perturbatively interacting gas of deconfined quarks and gluons. It was expected to be reached above the critical temperature $T_c \sim 170$ MeV [3–6], where the rapid increase of the effective number of active degrees of freedom $[\varepsilon(T)/T^4]$ was found in lattice QCD simulations [7,8]. Nowadays it is clear that such a state will be reached only at significantly higher temperatures than those accessible today. For temperatures a few times higher than the critical temperature T_c, the interactions and correlations in the hot QCD matter are still strong (e.g., see Refs. [9,10]), the recent term for it being strongly coupled QGP (sQGP) [10].

Critical assessments of hot QCD physics, e.g. Ref. [2], stress the present absence of, and the need for, a direct, compelling ''smoking gun'' signal for production of a new form of matter in RHIC collisions. The most compelling ''smoking gun'' would be a restoration of the symmetries of the QCD Lagrangian in hot, dense matter, notably the [$\mathrm{SU}_A(3)$ flavor] chiral symmetry and the $\mathrm{U}_A(1)$ symmetry, which are broken in the vacuum.

Among the issues pointed out as important was also the need to clarify the role of quark-antiquark ($q\bar{q}$) bound states continuing to exist above the critical temperature T_c [2]. Namely, evidence is accumulating that strong correlations in the form of quark-antiquark ($q\bar{q}$) bound states and resonances still exist [9,11] in the sQGP above the critical temperature. While in the old paradigm even deeply bound charmonium ($c\bar{c}$) states such as J/Ψ and η_c were expected to dissociate at $T \approx T_c$, the behavior of their spectral functions as extracted by the maximum entropy method [12] from lattice QCD simulations of mesonic correlators now indicates that they should persist till around $2T_c$ [13,14] or even above [15]. There are similar indications for light-quark mesonic bound states from lattice QCD [16] and from other methods [9,17]. This motivates their study in the framework of relativistic bound-state equations, i.e., the Poincaré-covariant Dyson-Schwinger (DS) approach to quark-hadron physics [18–21], which is a continuous approach complementary to lattice QCD studies. The DS approach is especially valuable in the light-quark sector, where chiral symmetry is essential. Namely, the DS approach is unique in that it can incorporate the correct chiral behavior of QCD, unlike other bound-state approaches. This is because the crucial low-energy QCD phenomenon of dynamical chiral symmetry breaking (DChSB) is well understood and under control in the DS approach [18–21], at least in the consistent rainbow-ladder approximation (RLA), where kernel *Ansätze* of the form

$$K(p)^{hg}_{ef} = -g^2 D^{\mathrm{eff}}_{\mu\nu}(p)\left[\frac{\lambda^a}{2}\gamma_\mu\right]_{eg}\left[\frac{\lambda^a}{2}\gamma_\nu\right]_{hf} \qquad (1)$$

(where e, f, g, h schematically represent spinor, color, and flavor indices) are used for the interactions between quarks in both Eq. (2), the gap equation $S^{-1} = S_0^{-1} - \Sigma$ for the full, dressed quark propagator S (S_0 is the free, bare one),

*davorh@phy.hr
†Corresponding author.
‡klabucar@oberon.phy.hr
§aradzh@theor.jinr.ru

and the Bethe-Salpeter (BS) equation (3) for the meson quark-antiquark bound state $\mathcal{M}$. That is, in RLA, the full propagator of the quark of the flavor q characterized by the bare mass $\tilde{m}_q$ is given by

$$S_q(p)^{-1}_{ef} = [\mathrm{i}\gamma\cdot p + \tilde{m}_q]_{ef} + \int S_q(\ell)_{gh} K(p-\ell)^{hg}_{ef} \frac{d^4\ell}{(2\pi)^4} \tag{2}$$

(in Euclidean space), while the bound-state vertex $\Gamma_{\mathcal{M}} = \Gamma_{q\bar{q}'}$ of the meson $\mathcal{M}$ composed of the quark q and antiquark $\bar{q}'$ is

$$\Gamma_{q\bar{q}'}(k,p)_{ef} = \int \left[S_q\left(\ell + \frac{p}{2}\right) \Gamma_{q\bar{q}'}(\ell,p) S_{q'}\left(\ell - \frac{p}{2}\right) \right]_{gh} \times K(k-\ell)^{hg}_{ef} \frac{d^4\ell}{(2\pi)^4}. \tag{3}$$

In the above equations, integrations are over loop momenta, and $D^{\mathrm{eff}}_{\mu\nu}(p)$ is an effective gluon propagator which, at the present stage of DS studies [18–21], must be modeled in the nonperturbative QCD regime for *low* momenta, $p^2 \lesssim 1\ \mathrm{GeV}^2$.

In the DS approach, all light pseudoscalar mesons ($\pi^{0,\pm}$, $K^{0,\pm}$, $\bar{K}^0$, η) manifest themselves *both* as quark-antiquark ($q\bar{q}$) bound states *and* (almost-)Goldstone bosons of DChSB, which also generates the condensates and the weak decay constants of the right magnitude, rather independent of the small current quark masses $\tilde{m}_q$, which can even be vanishing, as $\tilde{m}_q = 0$ corresponds to the chiral limit. For reviews, see, e.g., Refs. [18–21]. Reference [18] also reviews the studies of QCD DS equations at $T > 0$, which were started in [22].

The restoration of the chiral symmetry should take place at the temperature T_{Ch}, which is expected to be close or maybe even equal to the critical temperature T_c (e.g., see Refs. [23–25]). Most scenarios expect the restoration of the $\mathrm{U}_A(1)$ symmetry as the topological susceptibility melts with temperature. Such a situation calls for a good understanding, especially of the light pseudoscalar nonet, where pions and kaons to an excellent approximation, and η and η' to a good approximation, are eigenstates of flavor SU(3). However, for the neutral states with hidden strangeness, this will change if the gluon-anomaly contribution melts with temperature. The most interesting effects were predicted for η and η'. Their production rates were predicted to be enhanced [26,27], because their masses were expected to fall with T as the restoration of the $\mathrm{U}_A(1)$ symmetry takes place. However, for understanding such signatures, pseudoscalar meson masses (especially m_η and $m_{\eta'}$) at $T > 0$ must be better understood. The present paper contributes to this by extending to finite temperatures the successful bound-state, DS approach of Refs. [28–31] to the η-η' complex.

This paper is organized as follows. In the next section we introduce briefly the chosen dynamical model, but also explain generally how in the DS approach one can construct the mass eigenstates in the η-η' complex, be it at $T = 0$ or $T > 0$. In the third section, the topological susceptibility is related to the anomalous part of the η and η' masses, and its temperature dependence fitted. Section IV explains why various relationships between chiral and $\mathrm{U}_A(1)$ symmetries would lead to different temperature evolutions of the η-η' complex, and Sec. V gives the T dependence of pseudoscalar masses for various scenarios. We summarize in the last section.

II. PSEUDOSCALAR MESONS AT $T \geq 0$

A. The model and its results in the nonanomalous sector

The non-Abelian ("gluon") QCD axial anomaly is essential for the η-η' complex. References [28–31] show how to incorporate the effects of the anomaly into the DS approach and achieve a successful description of η and η' (at $T = 0$). They also show [28–31] that this works if one first achieves what is needed for the *nonanomalous* aspect of the η-η' complex, namely, the good description of pions and kaons. While the DS approach in RLA tackles this efficiently at $T = 0$, it is technically quite difficult to extend solving Eqs. (1)–(3) to nonvanishing temperatures. We thus adopt a simple model for the strong dynamics, the *separable interaction* [32]:

$$g^2 D^{\mathrm{eff}}_{\mu\nu}(p-\ell) \longrightarrow \delta_{\mu\nu} D(p^2, q^2, p\cdot q), \tag{4}$$

$$D(p^2,\ell^2,p\cdot\ell) = D_0 \mathcal{F}_0(p^2)\mathcal{F}_0(\ell^2) + D_1 \mathcal{F}_1(p^2)(p\cdot\ell)\mathcal{F}_1(\ell^2). \tag{5}$$

This is an interaction with the two strength parameters, D_0 and D_1, and simply modeled form factors

$$\mathcal{F}_0(p^2) = \exp(-p^2/\Lambda_0^2), \tag{6}$$

$$\mathcal{F}_1(p^2) = \frac{1+\exp(-p_0^2/\Lambda_1^2)}{1+\exp((p^2-p_0^2)/\Lambda_1^2)}, \tag{7}$$

also used in the calculations at $T \geq 0$ in Refs. [33–35], where fitting the properties of nonstrange (NS) mesons, containing just u and d quarks, fixed the parameters to

$$\Lambda_0 = 758\ \mathrm{MeV}, \qquad \Lambda_1 = 961\ \mathrm{MeV}, \qquad p_0 = 600\ \mathrm{MeV}, \tag{8}$$

$$D_0\Lambda_0^2 = 219, \qquad D_1\Lambda_0^4 = 40, \tag{9}$$

which we also adopt here without any further refitting. As in Refs. [32–35], the Matsubara formalism is used for calculations at $T > 0$. The usage of the above separable model interaction greatly simplifies DS equations and calculations at finite T, while yielding equivalent results on a given level of truncation [32,36], and a similar quality of results for pions [32,33] and now also for kaons [34]

(and fictitious $s\bar{s}$ pseudoscalars) at $T = 0$ as in Refs. [28–31], which employ more realistic interactions while modeling QCD. Most of the presently pertinent results of Ref. [34] of the separable model at $T = 0$ are summarized in Table I. In addition, also important are the chiral-limit value of the $\bar{q}q$ condensate, $\langle\bar{q}q\rangle_0 = (-217\ \mathrm{MeV})^3$, and the chiral-limit value of the pion decay constant, $f_\pi^0 = 89$ MeV. They agree well with the values appropriate for QCD in the chiral limit [37,38]. The important aspect of the good chiral behavior is that the pseudoscalar masses obey the Gell-Mann-Oakes-Renner–type relation

$$M^2_{q\bar{q}'} = \mathrm{const}(\tilde{m}_q + \tilde{m}_{q'}), \tag{10}$$

as in all consistently formulated DS approaches, where Eq. (10) is an excellent approximation even for realistically heavy strange quarks, so that the mass of the unphysical $s\bar{s}$ pseudoscalar can be expressed as

$$M^2_{s\bar{s}} = 2M^2_K - M^2_\pi \tag{11}$$

[e.g., the results in Table I obey Eq. (11) up to $\frac{1}{4}\%$].

Solving [34] Eq. (3) yields the masses M_π, M_K, and $M_{s\bar{s}}$, and the BS vertices $\Gamma_{q\bar{q}'}$. The meson decay constants $f_{q\bar{q}'}$ (e.g., $f_{u\bar{s}} = f_K$) can then be calculated as

$$f_{q\bar{q}'} p_\mu = N_c\,\mathrm{tr_s} \int \frac{d^4\ell}{(2\pi)^4}\,\gamma_5\gamma_\mu S_q\!\left(\ell + \frac{p}{2}\right) \times \Gamma_{q\bar{q}'}(\ell; p) S_{\bar{q}'}\!\left(\ell - \frac{p}{2}\right). \tag{12}$$

These calculations were extended to $T > 0$. To save space, the temperature-dependent masses of the pseudoscalars π, K and the $s\bar{s}$ are not displayed in a separate figure, but together with the anomalous masses from the η-η' complex in Fig. 1 [and in Figs. 5–9 further below, showing the same $M_\pi(T)$, $M_K(T)$, and $M_{s\bar{s}}(T)$, just for variously scaled relative temperatures].

TABLE I. Results (in GeV) on the nonanomalous pseudoscalar mesons for $T = 0$: masses M_P and decay constants f_P of the pseudoscalar $q\bar{q}'$ bound states $P = \pi$, K and unphysical $s\bar{s}$. The corresponding constituent masses are $m_u(0) = 0.398$ GeV and $m_s(0) = 0.672$ GeV; the chiral-limit condensate is $-\langle q\bar{q}\rangle_0 = (0.217)^3$ GeV^3. All results are obtained for the bare quark masses $\tilde{m}_{u,d} = 5.5$ MeV and $\tilde{m}_s = 115$ MeV and the effective interaction parameter values (8) and (9), fixed in our Refs. [34,35]. These masses and decay constants are the input for the description of the η-η' complex. [Later, in Eq. (16), we will name the unphysical $s\bar{s}$ pseudoscalar meson η_S, but note that the mass M_{η_S} (21), introduced in the NS–S mass matrix (17), includes the contribution from the gluon anomaly, whereas $M_{s\bar{s}}$ does not.]

P	M_P	M_P^{exp}	f_P	f_P^{exp}
π	0.140	0.1396	0.092	0.0924 ± 0.0003
K	0.495	0.4937	0.110	0.1130 ± 0.0010
$s\bar{s}$	0.685		0.119	

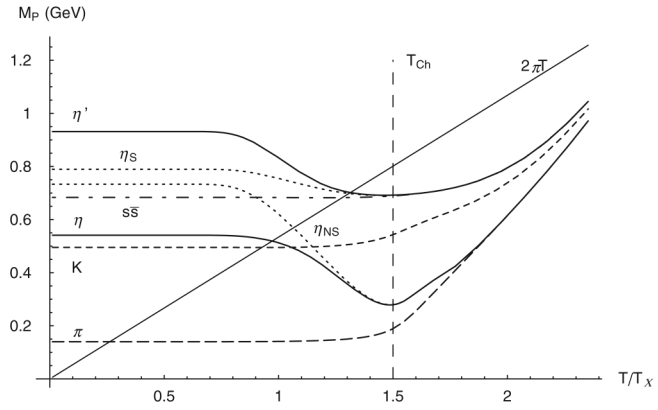

FIG. 1. The dependence of the pseudoscalar meson masses on the relative temperature T/T_χ, where the temperature scale (characterizing η-η' behavior) is, for illustrative purposes, temporarily chosen to be (unrealistic) $T_\chi = 2/3T_{\mathrm{Ch}} = 0.667T_{\mathrm{Ch}}$. The chiral restoration temperature T_{Ch} is marked by the thin-dashed vertical line. The masses which do not receive contributions from the gluon anomaly, $M_\pi(T)$, $M_K(T)$, and $M_{s\bar{s}}(T)$, are depicted by the long-dashed, short-dashed, and dash-dotted curves, respectively. They practically do not change with temperature till $T \approx 0.95T_{\mathrm{Ch}}$, after which they rise monotonically towards the thin diagonal line, which (in all figures displaying masses) represents twice the zeroth Matsubara frequency, $2\pi T$. This is the limit to which meson masses should ultimately approach from below at still higher temperatures, where $q\bar{q}$ states should totally dissolve into a gas of weakly interacting quarks and antiquarks. The masses in the η-η' complex exhibit different behavior due to the gluon anomaly, as will be explained below: the lower solid curve is $M_\eta(T)$, and the upper solid curve is $M_{\eta'}(T)$. The lower and upper dotted curves are, respectively, the η_{NS} and η_S masses.

Figure 2 gives the T dependences of the decay constants for the realistic explicit chiral symmetry breaking, but also $f_\pi^0(T)$, the chiral-limit version of $f_\pi(T)$. Its behavior precisely shows the value of the chiral symmetry restoration temperature T_{Ch}, because $f_\pi^0(T)$ vanishes at $T = T_{\mathrm{Ch}}$, as does the chiral condensate $\langle\bar{q}q(T)\rangle_0$. We also confirm [33] the result of earlier DS studies at finite T [39] that the *scalar* σ meson becomes degenerate with the pion after this temperature T_{Ch}; in the chiral limit its mass $M_\sigma(T)$ in fact tends to zero as $T \to T_{\mathrm{Ch}}$ [similarly as $f_\pi^0(T)$], as it should be at the chiral restoration.

Besides all these correct, very advantageous behaviors, there is the disadvantage that in the model used in Refs. [34,35] and in the present paper, we find the value $T_{\mathrm{Ch}} = 128$ MeV, which is significantly lower than the values (167–188 MeV) indicated by various lattice QCD studies [40]. This is a well-known drawback of the rank-2 separable DS model [32], but its low chiral symmetry restoration temperature can be raised by coupling the Polyakov loop variable to the quark sector [41]. This approach is currently under consideration [42]. More importantly, note that in the present paper we do not address

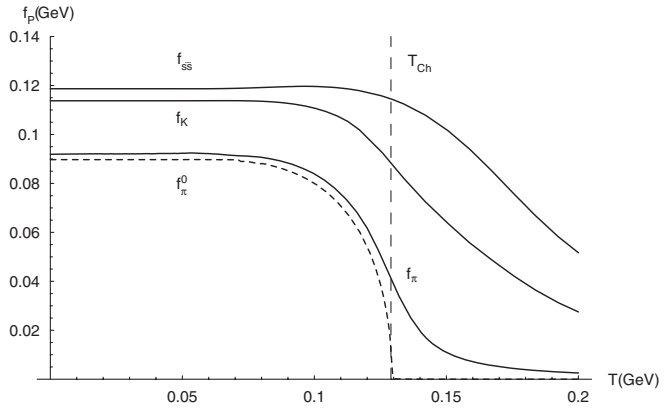

FIG. 2. The temperature dependence of the pseudoscalar meson decay constants, $f_\pi(T)$, $f_K(T)$, and $f_{s\bar{s}}(T)$. We observe the typical crossover behavior. Even for the purely nonstrange pseudoscalar, the pion, $f_\pi(T)$ does not fall to zero for the realistically small but nonvanishing explicit breaking of chiral symmetry, although the decrease of $f_\pi(T)$ is very strong around $T = T_{\rm Ch}$, where it would even vanish in the chiral limit (i.e., if $\tilde{m}_q \to 0$), as shown by the dashed curve representing the chiral-limit pion decay constant $f_\pi^0(T)$. Increased explicit breaking of chiral symmetry due to s quarks lessens temperature dependence, as shown by $f_K(T)$ and $f_{s\bar{s}}(T)$.

quantitative predictions at some specific absolute temperature; rather, as will become clear in detail in Sec. IV, we are interested in the dependence on the *relative* temperature, since we will study various scenarios for various ratios between the chiral restoration temperature $T_{\rm Ch}$ and the temperature scale T_χ characterizing the disappearance of the gluon anomaly. For this, the present model is adequate in spite of relatively low $T_{\rm Ch}$.

In summary, the nonanomalous physics is all modeled successfully [34,35] for the present purposes, and is ready to serve as input for constructing η and η'.

B. The anomalous sector: η-η' complex at $T \geq 0$

The construction of physical meson states in the present model starts as in Refs. [28–31]. Be it at $T = 0$ or $T > 0$, solving of the BS equations yields quark-antiquark bound-state solutions and the eigenvalues of the squared masses; e.g., $M^2_{u\bar{s}} = M^2_K$, as the pseudoscalar $u\bar{s}$ state is simply the positive kaon K^+. By their strangeness and/or charge, such $q\bar{q}'$ states (where $q' \neq q$) are protected from mixing with the hidden flavor $q\bar{q}$ states $u\bar{u}$, $d\bar{d}$, $s\bar{s}$, for which BS equations yield the masses $M^2_{u\bar{u}}$, $M^2_{d\bar{d}}$, $M^2_{s\bar{s}}$. Although the mass matrix of the light hidden flavor pseudoscalars is already diagonal in the basis $u\bar{u}$-$d\bar{d}$-$s\bar{s}$,

$$\hat{M}^2_{NA} = \mathrm{diag}[M^2_{u\bar{u}}, M^2_{d\bar{d}}, M^2_{s\bar{s}}], \tag{13}$$

the states $u\bar{u}$, $d\bar{d}$, $s\bar{s}$ do not correspond to any physical particles—certainly not to the isospin eigenstates π^0, η, and η', the neutral flavorless pseudoscalars found experimentally at $T = 0$. Although $M^2_{u\bar{u}} = M^2_{d\bar{d}} = M^2_\pi$ *in the isospin limit*, $M^2_{u\bar{u}}$, $M^2_{d\bar{d}}$, $M^2_{s\bar{s}}$ do not *automatically* represent any physical masses, at least not at $T = 0$, since $\hat{M}^2_{NA}$ is only the *nonanomalous* (NA) part of the complete mass matrix $\hat{M}^2 = \hat{M}^2_{NA} + \hat{M}^2_A$. Its *anomalous* part $\hat{M}^2_A$, the only nonvanishing one in the chiral limit, in the basis $u\bar{u}$-$d\bar{d}$-$s\bar{s}$ reads

$$\hat{M}^2_A = \beta \begin{bmatrix} 1 & 1 & 1 \\ 1 & 1 & 1 \\ 1 & 1 & 1 \end{bmatrix} \underset{\text{breaking}}{\overset{\text{flavor}}{\longrightarrow}} \beta \begin{bmatrix} 1 & 1 & X \\ 1 & 1 & X \\ X & X & X^2 \end{bmatrix}, \tag{14}$$

where the first matrix neglects the influence of the SU(3) flavor symmetry breaking, while the second is its modification which takes this into account as follows. Equation (14) shows that, due to the gluon anomaly, there are transitions between the states $u\bar{u}$, $d\bar{d}$, and $s\bar{s}$. However, the amplitudes for the transitions from, and into, light pseudoscalar $u\bar{u}$ and $d\bar{d}$ pairs are expected to be different, namely, larger, than those for the significantly more massive $s\bar{s}$. To allow for the effects of the breaking of SU(3) flavor symmetry, we can write $\langle q\bar{q}|\hat{M}^2_A|q'\bar{q}'\rangle = b_q b_{q'}$, where $b_q = \sqrt{\beta}$ for $q = u$, d and $b_q = X\sqrt{\beta}$ for $q = s$. The most widely used estimate of the flavor breaking is the ratio of NS and S pseudoscalar decay constants, $X = f_\pi/f_{s\bar{s}}$ [29,31,43,44]. Since we compute both f_π and $f_{s\bar{s}}$, our X is a predicted quantity, and not a fitting parameter. Our present model result at $T = 0$, $f_\pi/f_{s\bar{s}} = 0.773$, is very close to $X_{\rm exp} \approx 0.779$ extracted phenomenologically, i.e., from the mass matrix featuring experimental meson masses—see Refs. [29,31].

In any case, the complete mass matrix $\hat{M}^2$ is very far from being diagonal in this basis, since phenomenology at $T = 0$ indicates [see $\beta_{\rm fit}$ below Eq. (24)] that $\beta \approx 0.3\ \mathrm{GeV}^2 \gg M^2_{u\bar{u}}, M^2_{d\bar{d}}$ (and $\beta \sim M^2_{s\bar{s}}$).

The basis suggested for neutral ($I_3 = 0$) mesons by the flavor SU(3) quark model, and especially by almost exact isospin symmetry, is the octet-singlet basis with well-defined isospin quantum numbers: the isovector ($I = 1$) pion $\pi^0 = (u\bar{u} - d\bar{d})/\sqrt{2}$ and the isoscalar ($I = 0$) etas $\eta_8 = (u\bar{u} + d\bar{d} - 2s\bar{s})/\sqrt{6}$, $\eta_0 = (u\bar{u} + d\bar{d} + s\bar{s})/\sqrt{3}$. In the case of the flavor-broken SU(3), this is the *effective* octet-singlet basis, in which the *complete* mass matrix $\hat{M}^2 = \hat{M}^2_{NA} + \hat{M}^2_A$ is rather close to diagonal in the familiar $T = 0$ case. That is, at zero temperature and for realistic flavor breaking, η is close to η_8 and η' to η_0, thanks to the presence of the gluon anomaly (and in the chiral limit, the only nonvanishing mass is that of η_0, then equal to 3β). In the DS approach, this is shown in detail (with all numerical values) in Ref. [31]. The present case is very similar, regardless of the different dynamical model used.

Therefore, the effective flavor-broken SU(3) states η_8 and η_0 will be close to the respective physical mesons η and η' as long as the gluon anomaly plays a similar role as at $T = 0$. However, vanishing of the anomaly ($\beta = 0$) at sufficiently high T would bring about the situation where

the no-anomaly limit of the neutral flavorless pseudoscalar states is $\pi^0 = u\bar{u}$, $\eta = d\bar{d}$, $\eta' = s\bar{s}$ (where even η' would be an almost-Goldstone boson). This, in principle, opens up the possibility to study the maximal isospin violation at high T [45,46], but as the effects of the small difference between u and d quark masses are not important for the present considerations, we stick to the isospin limit throughout the present paper. The pertinent states thus remain, even in the high-T limit, the combinations with well-defined isospin quantum numbers. As long as $u\bar{u}$ and $d\bar{d}$ are bound, π^0 is given by $(u\bar{u} - d\bar{d})/\sqrt{2}$ and is decoupled from mixing with the two isoscalar etas, for which the no-anomaly-limit states are given by the so-called NS–S basis of the $I = 0$ subspace:

$$\eta_{NS} = \frac{1}{\sqrt{2}}(u\bar{u} + d\bar{d}) = \frac{1}{\sqrt{3}}\eta_8 + \sqrt{\frac{2}{3}}\eta_0, \tag{15}$$

$$\eta_S = s\bar{s} = -\sqrt{\frac{2}{3}}\eta_8 + \frac{1}{\sqrt{3}}\eta_0. \tag{16}$$

The 2×2 submatrix of $\hat{M}^2 = \hat{M}^2_{NA} + \hat{M}^2_A$ pertinent to the masses in the η-η' complex, in this basis, reads

$$\begin{bmatrix} M_\pi^2 + 2\beta & \sqrt{2}\beta X \\ \sqrt{2}\beta X & M^2_{s\bar{s}} + \beta X^2 \end{bmatrix} \underset{\phi}{\rightarrow} \begin{bmatrix} M_\eta^2 & 0 \\ 0 & M^2_{\eta'} \end{bmatrix}, \tag{17}$$

where the indicated diagonalization is achieved by the NS–S mixing relations

$$\eta = \cos\phi\,\eta_{NS} - \sin\phi\,\eta_S, \qquad \eta' = \sin\phi\,\eta_{NS} + \cos\phi\,\eta_S. \tag{18}$$

The NS–S mixing angle ϕ, related to the (equivalent) effective η_8-η_0 mixing angle θ as $\theta = \phi - \arctan\sqrt{2} = \phi - 54.74°$, is given by

$$\tan 2\phi = \frac{2M^2_{\eta_S\eta_{NS}}}{M^2_{\eta_S} - M^2_{\eta_{NS}}} \equiv \frac{2\sqrt{2}\beta X}{M^2_{\eta_S} - M^2_{\eta_{NS}}}, \tag{19}$$

where, from the η-η' mass matrix (17),

$$M^2_{\eta_{NS}} = M^2_\pi + 2\beta, \tag{20}$$

$$M^2_{\eta_S} = M^2_{s\bar{s}} + \beta X^2 = M^2_{s\bar{s}} + \beta\frac{f_\pi^2}{f^2_{s\bar{s}}}. \tag{21}$$

The theoretical η and η' mass eigenvalues are

$$M^2_\eta = \tfrac{1}{2}[M^2_{\eta_{NS}} + M^2_{\eta_S} - \Delta_{\eta\eta'}], \tag{22}$$

$$M^2_{\eta'} = \tfrac{1}{2}[M^2_{\eta_{NS}} + M^2_{\eta_S} + \Delta_{\eta\eta'}], \tag{23}$$

where $\Delta_{\eta\eta'} \equiv \sqrt{(M^2_{\eta_{NS}} - M^2_{\eta_S})^2 + 8\beta^2X^2}$.

III. TOPOLOGICAL SUSCEPTIBILITY AND η, η'

In the nonanomalous pseudoscalar meson sector, we calculated M_π, $M_{s\bar{s}}$, f_π, $f_{s\bar{s}}$, and X at zero and nonvanishing temperatures [34]. Except for the anomalous contribution β, this is everything one needs for computing, at $T = 0$ and $T > 0$, the mixing angle (19) and our predictions for the masses in the η-η' complex. But, the anomaly effects, including β, obviously cannot be calculated in the present DS approach utilizing the ladder approximation. Fortunately, since the gluon anomaly is suppressed as $1/N_c$ in the expansion in the number of colors N_c, it was shown that considering the gluon-anomaly effect only at the level of mass shifts and neglecting its effects on the bound-state solutions is a meaningful approximation [28,29,31]. Thus, in the present paper we also avoid the $U_A(1)$ problem by breaking nonet symmetry just at the level of the masses, adding by hand the anomaly contribution $\hat{M}^2_A$ to the calculated nonanomalous mass matrix $\hat{M}^2_{NA}$ to form the total mass matrix $\hat{M}^2$. From the traces in Eq. (17),

$$\beta = \frac{1}{2 + X^2}[M^2_\eta + M^2_{\eta'} - M^2_\pi - M^2_{s\bar{s}}], \tag{24}$$

where M_π, $M_{s\bar{s}}$, and $X = f_\pi/f_{s\bar{s}}$ are already calculated quantities (see Table I), whereas M_η and $M_{\eta'}$ remain to be determined.

One may treat β as a fitting parameter and fix it by requiring $M^2_\eta + M^2_{\eta'} = (M^2_\eta)_{\rm exp} + (M^2_{\eta'})_{\rm exp} = 1.2169\ {\rm GeV}^2$ in Eq. (24), yielding $\beta_{\rm fit} = 0.282\ {\rm GeV}^2$.

However, one can avoid treating β as a new fitting parameter, since it can be extracted from the lattice. Using Eq. (11) in Eq. (24) gives the first equality in

$$\beta(2 + X^2) = M^2_\eta + M^2_{\eta'} - 2M^2_K = \frac{6}{f^2_\pi}\chi. \tag{25}$$

The second equality in Eq. (25) is the Witten-Veneziano (WV) relation [47,48] between the η, η' and kaon masses and χ, the topological susceptibility of the pure Yang-Mills gauge theory ($\chi = \chi_{\rm YM}$).

The lattice results ($\chi_{\rm latt}$) on χ imply through Eq. (25)

$$\beta_{\rm latt} = \frac{1}{2 + X^2}\frac{6}{f^2_\pi}\chi_{\rm latt}. \tag{26}$$

Taking for $\chi_{\rm latt}$ the central value of the weighted average,

$$\chi(T = 0) = (175.7 \pm 1.5\ {\rm MeV})^4, \tag{27}$$

of the recent lattice results on the topological susceptibility [49–51] at $T = 0$ gives $\beta_{\rm latt} = 0.260\ {\rm GeV}^2$.

Table II summarizes our $T = 0$ results on η and η'. The agreement with the experimental masses is excellent for both $\beta = \beta_{\rm fit}$ and $\beta = \beta_{\rm latt}$. In the latter case, there is not even one new parameter introduced in addition to the parameters already fixed in the nonanomalous, π and K sector. The case $\beta = \beta_{\rm latt}$ is especially satisfying because the lattice results for the topological susceptibility χ also

TABLE II. The η and η' masses and mixing angle at $T = 0$, and comparison with experiment, for the cases $\beta = \beta_{\rm fit} = 0.282$ GeV^2 and $\beta = \beta_{\rm latt} = 0.260$ GeV^2. For both cases, the input from the nonanomalous sector is the same: $X = 0.773$ and M_π and $M_{s\bar{s}}$ from Table I. All masses M_η, $M_{\eta'}$, $M_{\eta_{NS,S,8,0}}$, and $\sqrt{3\beta}$ are in MeV. The purely anomalous mass $\sqrt{3\beta}$ is the mass of η' in the chiral limit for all three flavors, where η is massless together with the other octet pseudoscalars. In the chiral limit, as well as the exact flavor SU(3) limit, $\phi = \arctan\sqrt{2}$, i.e., $\theta = 0$, so that $\eta' = \eta_0$ and $\eta = \eta_8$.

	$\sqrt{3\beta}$	$M_{\eta_{NS}}$	M_{η_S}	M_{η_8}	M_{η_0}	ϕ	M_η	$M_{\eta'}$
$\beta_{\rm fit}$	919.5	763.7	798.0	574.3	944.2	42.51°	548.9	958.5
$\beta_{\rm latt}$	884.0	735.2	790.0	573.7	914.8	40.82°	543.1	932.5
Experiment							547.7	957.8

exist for $T > 0$ [52,53], and can be used to express $\beta(T > 0)$ and study the η-η' complex also at nonvanishing temperatures, if we assume that the WV relation continues to hold at $T > 0$ as well.

Various lattice results [52] on the topological susceptibility $\chi(T)$ are fitted well by the following expression,

$$\chi(T) = \chi(0)\left\{\exp\left[\left(\frac{T}{T_\chi}\right)^\kappa - \kappa^\alpha\left(\frac{T_\chi}{T}\right)^\kappa\right] + 1\right\}^{-\delta}, \quad (28)$$

depending on the *relative* temperature T/T_χ, where T_χ is the characteristic (''melting'') temperature where $\chi(T)$ starts decreasing appreciably.

For $\kappa = 4.2$, $\alpha = 0.2$, and $\delta = 0.76$ (solid curve in Fig. 3), Eq. (28) fits well the lattice data [52] on the pure Yang-Mills topological susceptibility, $\chi(T) = \chi(T)_{\rm YM}$, which is the one consistent to use in the WV relation. However, we will also be interested in fitting the shape of $\chi(T)/\chi(0)$ for the SU(3) quenched QCD data [dashed curve in Fig. 3, obtained with $\kappa = 5.1$, $\alpha = 0.5$, and $\delta = \kappa/4$ in Eq. (28)], as well as that shape for the case of the four-flavor QCD lattice data [52] (dotted curve in Fig. 3, obtained with $\kappa = 13$, $\alpha = 0.5$, and $\delta = 2.4$).

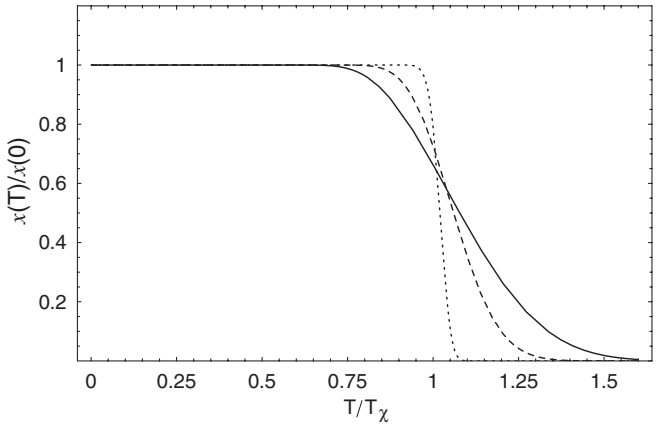

FIG. 3. The relative topological susceptibility $\chi(T)/\chi(0)$ given by Eq. (28) fitting the lattice data [52] for the three cases: pure Yang-Mills (solid curve, the slowest melting rate), SU(3) quenched (dashed curve, intermediate melting rate), and four-flavor QCD (dotted curve, the fastest melting rate).

One extreme behavior of the topological susceptibility, qualitatively described by Eq. (28) for low values of T_χ, is the most traditional scenario, due to Pisarski and Wilczek [54] and studied, e.g., by Ref. [27]. Now, however, it appears to be disfavored, as then $\chi(T)$ melts away with T rather quickly, since one supposes that $\chi(T)$ is due to the instanton contribution which decreases exponentially as the so-called ''Pisarski-Yaffe suppression factor'' [55]. Then, T_χ would be significantly below $T_{\rm Ch}$, which may be judged too unrealistic to consider [56]. Still, we consider it for illustrative purposes, since in the present bound-state approach in conjunction with $\chi(T) = \chi(T)_{\rm YM}$, one can get falling masses and enhanced η and η' production (predicted by, e.g., Refs. [26,27]) only in this case, and for $T_\chi = T_{\rm Ch}$ but with $\chi(T)$ falling much more sharply than $\chi(T)_{\rm YM}$, as will be shown below.

The opposite extreme possibility is $\chi(T) \approx$ const; i.e., $U_A(1)$ symmetry is not restored around the critical temperature, but at much higher, possibly infinite T (e.g., see Ref. [57]). This possibility is approached by Eq. (28) for growing T_χ.

At zero temperature, η_{NS} and η_S are almost as ''misaligned'' with η and η' as they can be, as shown by our NS–S mixing angle close to $\phi \approx 45°$. This must be so for any successful model, since it is mandated by phenomenology at $T = 0$, as seen, e.g., in Ref. [31]. But, if the topological susceptibility vanishes when T becomes large enough, $\beta \to 0$ causes $\phi \to 0$ in the end, along with $\eta \to \eta_{NS}$, $\eta' \to \eta_S$ and $M_\eta \to M_\pi(T)$, $M_{\eta'} \to M_{s\bar{s}}(T)$. Depending on how the mass contribution of the gluon anomaly varies with growing T, various interesting effects can occur before this limit is reached.

IV. CHIRAL VS. $U_A(1)$ SYMMETRY RESTORATION AT $T > 0$

The temperature evolution of the η-η' mass matrix (17) results from the T dependence not only of χ, but also of f_π, $f_{s\bar{s}}$, M_π, and $M_{s\bar{s}}$. As shown by Eq. (25), the ratio $\chi(T)/f_\pi(T)^2$ is crucial for the T dependence of the anomalous mass contribution.

Thus, contrary to the assumptions often made in the literature (e.g., Ref. [58]), the decrease of the topological susceptibility does not imply *automatic* restoration of $U_A(1)$ symmetry (e.g., see Ref. [59]). We will see that the assumption that it does is correct only if χ falls sufficiently faster than f_π^2, so that $\chi(T)/f_\pi^2(T)$ falls towards zero as T grows. We should thus explore what happens for various possible relationships between T_χ and $T_{\rm Ch}$, the respective temperatures of the onset of the fast decrease of $\chi(T)$ and of $f_\pi(T)$.

Many papers addressing the relationship of restoration of the chiral vs. $U_A(1)$ symmetry, e.g., Refs. [27,58,59], consider only one value of the temperature characterizing the melting of $\chi(T)$. Those of them [58,59] using the lattice results of Ref. [52] on the T dependence of χ do not employ the rather high susceptibility melting temperature (260 MeV) of that reference. They adopt the view of Ref. [52] that this temperature (T_χ in *our* notation) is the critical temperature T_c, but *rescale* the lattice results [52] for $\chi(T)$ to a lower value, $T_c = T_\chi = 150$ MeV. (This is in the ballpark appropriate to the full QCD, but significantly lower than the pure Yang-Mills case, where χ consistent with the WV relation is computed.) Rescaling of T_χ is also relevant for us, since we are interested in the dependence on *relative* temperature; i.e., we study various relationships between T_χ and $T_{\rm Ch}$. Below, we exhibit the case $T_\chi = T_{\rm Ch}$ as well as the cases when T_χ is roughly 15% and 30% below and above $T_{\rm Ch}$.

Recall that the present DS model gave us $T_{\rm Ch} = 128$ MeV for the chiral restoration temperature. This is lower than lattice results, since the lattice finds that $T_{\rm Ch}$ seems to coincide with the critical temperature T_c [23–25] and presently estimates T_c to be between 167 and 188 MeV for $2 + 1$ flavor QCD [40]. Nevertheless, our results have a more generic meaning than working in this simple model would indicate at first glance; using a more realistic interaction in the DS approach, such as in Ref. [39], gives $T_{\rm Ch}$ above 150 MeV, but the results obtained there otherwise look similar to the corresponding results here, just rescaled to the higher $T_{\rm Ch}$. Notably, Ref. [39] also found that $f_\pi(T)$ and $M_\sigma(T)$, vanishing at $T = T_{\rm Ch}$ in the chiral limit, do not vanish any more when the explicit breaking of chiral symmetry is introduced, but exhibit a crossover, just as we find in the present model. Also, the pseudoscalar meson mass exhibits very little variation below $T_{\rm Ch}$ [39], just as the π, K, and $s\bar{s}$ masses here. The main change is thus pushing the falloff behavior of $f_\pi(T)$, which happens around $T_{\rm Ch}$, to higher temperatures. The temperature-induced changes in the η-η' complex are thus given essentially by $2\beta(T) \sim 4\chi(T)/f_\pi^2(T)$ and $\beta(T)f_\pi^2(T)/f_{s\bar{s}}^2(T) \sim 2\chi(T)/f_{s\bar{s}}^2(T)$ [see Eqs. (20) and (21)]. Figure 2 shows that, unlike $f_\pi(T)$, $f_{s\bar{s}}(T)$ does not decrease by an order of magnitude across the examined T interval. Thus, the question of what decreases earlier, $\chi(T)$ or $f_\pi^2(T)$, and the related relationship between T_χ and $T_{\rm Ch}$, is what causes important, qualitative differences in T-evolution scenarios, and not what we happen to choose for our concrete dynamical model in the DS approach.

Let us note again here the advantage of the DS approach for analyzing the hot QCD matter in which $q\bar{q}$ bound states and/or resonances persist beyond the critical temperature marking not a real phase transition, but a relatively smooth crossover [10]. The DS approach enables the meaningful computation of quantities characterizing such bound states or resonances. For example, note that Fukushima *et al.* [59], who were the first to study the interplay of chiral symmetry restoration and melting of χ in the WV relation (25), use the Nambu-Jona-Lasinio (NJL) model (following, e.g., the pioneering papers [4,6]). However, the lack of confinement in the NJL model also leads to the disadvantage, important in the present context, that η' is not bound at all, not even at $T = 0$. It decays into quarks and antiquarks due to its large mass, so that $M_{\eta'}$ in the NJL model is not a well-defined quantity [59]. On the other hand, the present DS approach does not have such problems.

Another advantage of the DS approach is the behavior of $f_\pi(T)$. This approach has the correct chiral behavior also for finite T, so that $f_\pi(T)$ falls markedly at $T = T_{\rm Ch}$; but since the DS approach naturally also incorporates the effects of realistic explicit chiral symmetry breaking, $f_\pi(T)$ stays nonzero [18,39], albeit small, well beyond $T = T_{\rm Ch}$. This is in contrast to the chiral limit $f_\pi^0(T)$, where $f_\pi^0(T \geq T_{\rm Ch}) = 0$ precludes its usage in the WV relation for $T \geq T_{\rm Ch}$ (e.g., Ref. [59] or the studies [27,58,60] employing chiral Lagrangians).

V. RESULTS ON THE η-η' COMPLEX AT $T > 0$

A. Yang-Mills topological susceptibility

First, we explore the temperature dependence of the η-η' complex following from the usage of the pure Yang-Mills topological susceptibility, $\chi(T) = \chi(T)_{\rm YM}$, since it is the one consistent with the WV relation. One should keep in mind that the pure Yang-Mills case has the slowest T dependence, i.e., a significantly slower falloff than cases when quarks are present (see Fig. 3), which will motivate considering other cases in Sec. V B.

For illustrative purposes, let us begin with an unrealistically low χ-melting temperature, say $T_\chi = 2/3T_{\rm Ch}$. This is a representative case when the topological susceptibility $\chi(T)$ becomes very small well before $T_{\rm Ch}$, i.e., well before $f_\pi(T)$ can appreciably decrease. The temperature dependence of η and η' masses for this case is shown in Fig. 1. They remain practically as at $T = 0$, until $T \approx 0.9T_\chi$, after which the gluon-anomaly contributions start melting, and both $M_\eta(T)$ and $M_{\eta'}(T)$ start falling. After $T \approx 1.2T_\chi = 0.8T_{\rm Ch}$, we practically have $M_\eta(T) = M_{\eta_{NS}}(T)$ and $M_{\eta'}(T) = M_{\eta_S}(T)$, as η becomes pure η_{NS} and η' becomes pure η_S, and even pure nonanomalous $s\bar{s}$ after $T \approx 1.3T_\chi$. After $T = T_{\rm Ch}$, all masses rise, and η soon becomes degenerate with the pion.

This behavior is reflected in the mixing angle $\phi(T)$ which for the choice $T_\chi = 2/3T_{\rm Ch}$ just follows the topological susceptibility (28), falling monotonically from its $T = 0$ value to zero—see Fig. 4.

An important, potentially experimentally recognizable feature in Fig. 1 is the decrease of the masses of η', and especially of η. It starts well before $T = T_{\rm Ch}$, where the η mass is less than half of its $T = 0$ value. The decrease of the masses should result in an increase of their (especially

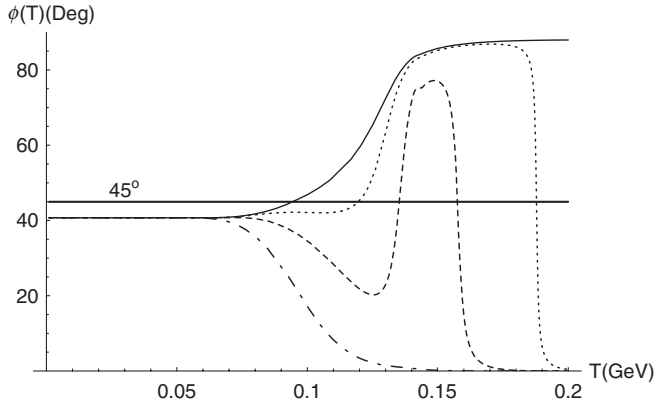

FIG. 4. The temperature dependence of the NS–S mixing angle ϕ for $T_\chi = 2/3T_{\rm Ch}$ (dash-dotted curve), $T_\chi = 0.758T_{\rm Ch}$ (dashed curve, the case not displayed in other figures), $T_\chi = 0.836T_{\rm Ch}$ (dotted curve), and $T_\chi = T_{\rm Ch}$ (solid curve). In all the cases, the pure Yang-Mills topological susceptibility is used in the WV relation (25).

η's) multiplicities. This case, with T_χ significantly lower than $T_{\rm Ch}$, thus illustrates well the T dependences of the masses of pseudoscalars in the Pisarski-Wilczek scenario [26,27,54].

Let us see how the behavior changes when T_χ is increased by, e.g., some 25%, to $T_\chi = 0.836T_{\rm Ch}$. Unlike in Fig. 1, $T = T_{\rm Ch}$ does not mark the onset of the approach to the asymptotic situation $[M_{\eta'}(T) \to M_{s\bar{s}}(T),\ M_\eta(T) \to M_\pi(T)]$. Now, in Fig. 5, $T = T_{\rm Ch}$ marks the strong increase of the η' mass, which almost doubles by $T/T_\chi \approx 1.4$, where it reaches its maximum and starts falling till its second, very narrow anticrossing with the η mass, which

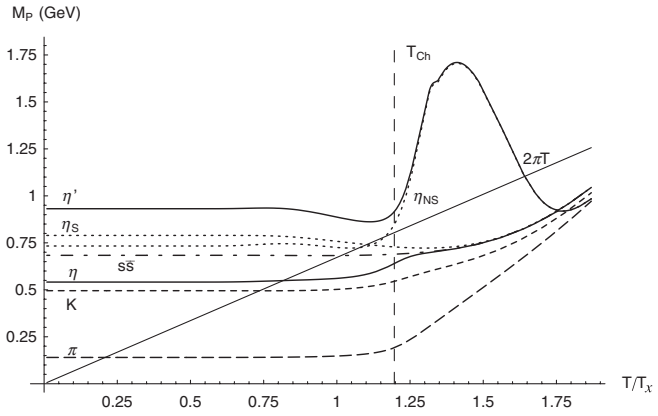

FIG. 5. The relative-temperature dependence, on T/T_χ, of the pseudoscalar meson masses for $T_\chi = 0.836T_{\rm Ch}$, i.e., $T_{\rm Ch} = 1.20T_\chi$, marked by the thin-dashed vertical line. The long-dashed, short-dashed, and dash-dotted curves again represent, respectively, $M_\pi(T)$, $M_K(T)$, and $M_{s\bar{s}}(T)$. The lower and upper solid curves are again $M_\eta(T)$ and $M_{\eta'}(T)$, respectively, and the lower and upper (except on a small segment) dotted curves are $M_{\eta_{NS}}(T)$ and $M_{\eta_S}(T)$.

just grows tamely and (almost) monotonically. [The crossings of η_{NS} and η_S correspond to the anticrossings of the η and η' masses (22) and (23).] The increase of T_χ also pushes the onset of the approach to the asymptotic situation beyond this second anticrossing.

This all happens because now the decrease of the pion decay constant $f_\pi(T)$ starts sufficiently before the decrease of the topological susceptibility, so that a large amplification of $\beta(T) \sim \chi(T)/f_\pi^2(T)$ occurs, and over a significant temperature interval. In contrast, $\beta(T)X(T)^2 \sim \chi(T)/f_{s\bar{s}}^2(T)$ is not so significantly enhanced. Equations (20), (21), and (25) show why $M_{\eta_{NS}}$ is larger than M_{η_S} in the interval $1.1T_\chi \lesssim T \lesssim 1.75T_\chi$ and is the largest contributor to $M_{\eta'}$. In the T interval where $M_{\eta_{NS}}(T)$ is significantly larger than other masses and $\beta(T)X(T)^2$, the expansion of $\Delta_{\eta\eta'}$ in Eq. (22) shows that the η mass is approximately the nonanomalous $s\bar{s}$ mass $M_{s\bar{s}}(T)$, with the gluon-anomaly contributions suppressed by $1/M_{\eta_{NS}}(T)$:

$$M_\eta^2 \approx M_{s\bar{s}}^2 - \frac{1}{2}\left[\frac{M_{s\bar{s}}^2}{M_{\eta_{NS}}} + \frac{\beta X^2}{M_{\eta_{NS}}}\right]^2 + \ldots. \qquad (29)$$

In this temperature interval, the heavier particle, η', is predominantly nonstrange, η_{NS}, while the lighter one, η, is mostly strange, η_S. Equation (19) shows that as $M_{\eta_{NS}}$ grows so does $\phi(T)$. It surpasses 45° when $M_{\eta_{NS}}$ surpasses M_{η_S}—compare Figs. 4 and 5. In fact, after $T \approx 1.25T_\chi = T_{\rm Ch}$, it climbs close to $\phi(T) \sim 90°$, as $\eta' \sim \eta_{NS}$ and $\eta \sim -\eta_S$. Then, as $\chi(T) \to 0$, $M_{\eta_{NS}}(T)$ falls back towards $M_\pi(T)$, and $\phi(T)$ falls [through 45° where again $M_{\eta_{NS}} = M_{\eta_S}$, while $M_{\eta'}(T)$ and $M_\eta(T)$ anticross] towards zero, and etas quickly reach their no-anomaly limit (15) and (16): $\eta = \eta_{NS}$ degenerate with the pion, and $\eta' = \eta_S$ with the nonanomalous mass $M_{s\bar{s}}(T)$.

The crucial role of the chiral restoration temperature $T_{\rm Ch}$ is already obvious. We assume next that the topological-susceptibility-melting temperature T_χ is still higher and equal to this temperature, i.e., $T_\chi = T_{\rm Ch}$. This case is illustrated in Fig. 6. It exhibits several interesting features. The most obvious one is such a strong increase of the η' mass that, soon after $T = T_{\rm Ch}$, it exceeds the scale of the figure. Of course, it does not indicate any divergence; after reaching the maximum value of around 5 GeV, $M_{\eta'}(T)$ falls down. It is just that the decreasing part of the $M_{\eta'}(T)$ curve below 1.6 GeV and the close η-η' anticrossing are pushed outside the examined temperature interval by widening of the interval where $M_{\eta_{NS}}(T)$ is enhanced. This results in the mixing angle $\phi(T)$, which in the displayed T interval ($T \leq 200$ MeV) does not return down from the value of approximately 90°; i.e., η' remains almost pure η_{NS}, and η almost pure η_S in the displayed T interval. The fall of $M_{\eta'}$ and approach to the no-anomaly asymptotic situation is thus postponed to higher temperatures now that we have increased T_χ, the "melting temperature" of the (anyway comparatively slowly decreasing) Yang-Mills χ. On the

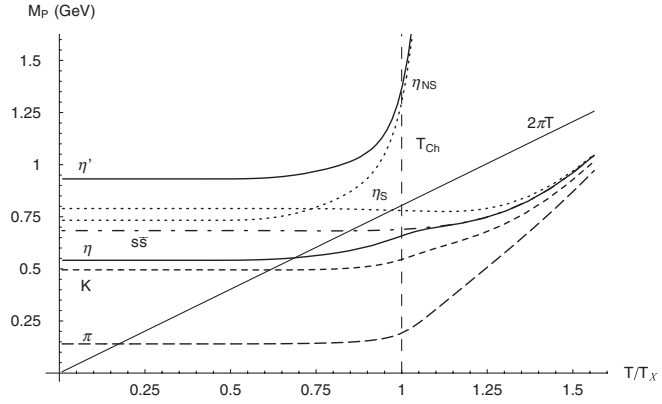

FIG. 6. The relative-temperature dependence, on T/T_χ, of the pseudoscalar meson masses for $T_\chi = T_{\rm Ch}$, marked by the thin-dashed vertical line. The meaning of all curves, lines, and other symbols is the same as in Figs. 1 and 5. The most conspicuous is the increase of $M_{\eta'}(T)$, which becomes as high as 5 GeV around $T = 1.3T_\chi$.

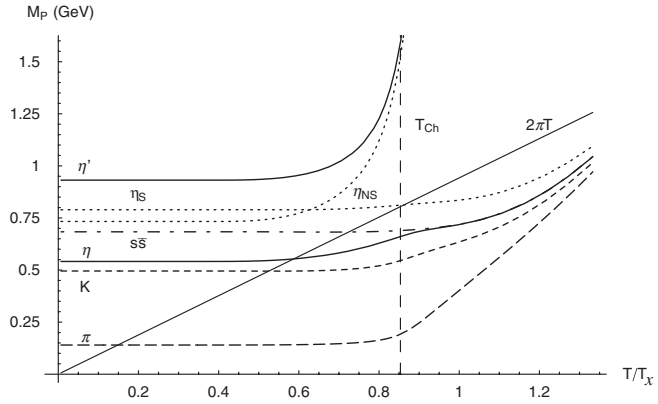

FIG. 7. The T/T_χ dependence of the meson masses for $T_\chi = 1.17T_{\rm Ch}$. The meaning of all symbols is again the same as in Figs. 1, 5, and 6. The increase of $M_{\eta'}(T)$ is huge, as high as 10 GeV around $T = 0.18$ GeV, since the masses in the η-η' complex are calculated (as in Figs. 1, 5, and 6, where T_χ is, however, lower) with the pure Yang-Mills topological susceptibility [52], which decreases comparatively slowly.

other hand, since the decrease of $f_\pi(T)$ is determined by $T_{\rm Ch}$, increasing T_χ lowers the value of the relative temperature where $M_{\eta_{NS}}(T)$ begins its fast climb.

All these features are readily understood on the basis of the detailed explanation of the previous case $T_\chi = 0.836T_{\rm Ch}$, but they are much more pronounced with respect to this case with just 16% lower T_χ. The described trends continue for $T_\chi > T_{\rm Ch}$. We illustrate this through the choice $T_\chi = 1.17T_{\rm Ch}$, which in our model corresponds to $T_\chi = 150$ MeV. This value is equal to T_χ and the critical temperature assumed, e.g., in the typical examples [27,58,59] of studies paralleling ours. These assumptions are obviously motivated by 150 MeV being roughly the value of the critical, transition temperature T_c found on the lattice for 3-flavor QCD [23].

The temperature behavior of the pseudoscalar meson masses for this case is shown in Fig. 7, and it is clear from the understanding gained on the previous choices of T_χ. The increase of the η and η' masses starts as early as $T/T_\chi = 0.6$, and, in the case of the η' mass, it is even more pronounced, the maximal $M_{\eta'}(T)$ being some 10 GeV. Its fall towards the $s\bar{s}$ mass (and the fall of the mixing angle from almost 90° to 0) is not seen in Fig. 7 since the approach to the asymptotic behavior happens at higher temperatures.

Let us summarize our findings from the WV relation used consistently with the pure Yang-Mills topological susceptibility: only very low, unrealistic values of T_χ, below some 70% of $T_{\rm Ch}$, would yield the drop in the η and η' masses which would allow the enhancement [26,27] of the η and η' production as in the Pisarski-Wilczek scenario. For all higher values of T_χ we found mostly increasing η and η' masses allowing no such enhancement in their production. The increase of the η mass in Figs. 5–7 is, however, moderate and relatively slow, so that in our qualitative treatment we do not venture to make any statement about a possible suppression of the η production either. In contrast to that, the enhancement of the η' mass is so dramatic for $T_\chi \gtrsim T_{\rm Ch}$ that one can argue that the η' production must be ever more suppressed for these values of T_χ—of course, provided that the η' mass increase observed in the present approach is at all genuine, and not an artifact.

B. Discussing caveats and probing other possibilities

While our bound-state approach, which includes both DChSB and realistic *explicit* ChSB, makes it possible to use the WV relation, and the pion decay constant in it, for the finite temperatures across the restorations of $U_A(1)$ and chiral symmetries, there is no guarantee that the WV relation does not ultimately fail at some T. Of course, it is not likely that the WV relation, after being a good approximation at lower T, should fail almost immediately after f_π starts falling with T. Thus, the behaviors of η and η' exhibited in the previous subsection should be considered at least as a serious qualitative indication that, e.g., some η' mass enhancement (and associated suppression of η' production) should exist at least over some T interval, even though the WV relation may break down after certain T. At this point, nevertheless, we must discuss and take into account the caveat that such a drastic η' mass increase (for $T_\chi \gtrsim T_{\rm Ch}$) suggests that it is in fact not a genuine effect, but at least to a large extent an artifact of our approximations and assumptions.

One can think of the large N_c approximation, in which the WV relation (with $\chi = \chi_{\rm YM}$) was derived, as a possible cause of unreliability of the WV relation after some T. The avenue towards improvement and better insight can then be

sought in the recent work by Shore [61,62], which contains what amounts to the generalization of the WV relation valid to *all orders* in $1/N_c$. Instead of the topological susceptibility χ, Shore's equations employ the full QCD topological charge parameter A (but since it is at present not known, Shore himself [61,62] had to approximate it by its lowest-order approximation in the $1/N_c$ expansion, namely, by the pure Yang-Mills topological susceptibility $\chi_{\rm YM}$). Also, besides f_π, the kaon decay constant and four different η and η' decay constants appear in Shore's pertinent equations (2.14)–(2.16) [61]. Equation (2.19) in Ref. [61] is also very illustrative, since after the $1/N_c$ expansion, it gives back the WV relation (25) as the lowest-order approximation. So, instead of the WV relation, Shore's generalization might be used in our bound-state approach. Indeed, this research has been initiated and is in progress [42], and there are already some preliminary results (notably at $T_\chi = T_{\rm Ch}$), but the presentation of this material is beyond the scope of the present paper. Nevertheless, already on the basis of the insights from the present work, we can and should make some comments on the indicative fact that the results from Shore's generalization at $T > 0$ are rather close [42] to our present results from the WV relation provided the same topological susceptibility χ is used instead of the full QCD topological charge parameter A.

It is instructive to compare the WV relation (25) with Shore's [61] Eq. (2.19). The refinement brought by the presence of the five additional decay constants in Shore's generalization (instead of just f_π, as in the WV relation) immediately suggests that the η' mass increase would not be as drastic as the ones obtained from the original WV relation for $T_\chi/T_{\rm Ch} \gtrsim 1$. Namely, these additional decay constants are all affected by the strange quarks; the way $f_{s\bar{s}}$ contributes to the η and η' decay constants can be seen in, e.g., Ref. [43] or the Appendix of Ref. [29]. Thus, they diminish with T slower than f_π, as shown in Fig. 2 for f_K and $f_{s\bar{s}}$. In keeping with that, our preliminary results indeed show that the η' mass increase is not as pronounced as in the present paper. However, the reduction is just about 20%, and, as already said, the results are on the whole rather similar. The refinement through the decay constants (other than f_π) thus improves, but does not really cure the suspicious η'-mass behavior. This indicates that the probable main problem is the usage of the topological susceptibility $\chi = \chi_{\rm YM}$ instead of the presently unknown full QCD topological charge parameter A. While the usage of the pure Yang-Mills topological susceptibility $\chi_{\rm YM}$ often turns out to be a reasonable approximation at $T = 0$ (e.g., see Refs. [28–31,43,61,62]), its "slow" temperature dependence contributes crucially to the perceived artifact of the present approach—the blowup of the η' mass. This motivates us to use the related topological susceptibilities obtained on the lattice [52] in the presence of quarks, namely, the SU(3) quenched and the four-flavor QCD case, as Fig. 3 shows that they "melt" faster. Thus, they hopefully provide a better approximation to the T dependence of the full QCD topological charge parameter, since we expect that, as usual, this quantity of the full QCD will be less resistant to the temperature-induced changes than the pure-glue, quarkless $\chi_{\rm YM}$.

In Fig. 8 we see the results for the SU(3) quenched QCD data, and in Fig. 9, the results for the four-flavor QCD data [as fitted by, respectively, the dashed and the dotted curves in Fig. 3, resulting from Eq. (28)].

In both figures, the same four values of the relative susceptibility melting temperatures $T_\chi/T_{\rm Ch}$ are used, as in the figures in the preceding subsection. Thus, in both Figs. 8 and 9, the four successive graphs starting from the top correspond to the four respective Figs. 1 and 5–7, which gave the T dependence for $\chi = \chi_{\rm YM}$. It was described in detail in the previous subsection, and on the basis of this we can easily understand the behavior of the masses in the new Figs. 8 and 9. What happens is that for the SU(3) quenched QCD, and especially for the four-flavor QCD, the topological susceptibility melts faster than in the pure Yang-Mills case, so that the patterns seen in the previous subsection for the pure Yang-Mills case are (roughly) reproduced at somewhat higher values of T_χ for the SU(3) quenched case, and even higher values of T_χ for the four-flavor case. Thus, the Pisarski-Wilczek scenario is realized in the upper two diagrams of Fig. 9 illustrating the four-flavor case, and just in the first diagram of Fig. 8. In any case we observe $M_\eta(T)$ quickly becoming degenerate with $M_\pi(T)$, before the chiral restoration temperature $T_{\rm Ch}$, while the behavior observed previously in Fig. 1 would now still be seen *well above* $T_\chi/T_{\rm Ch} = 2/3$. The second diagram from the top of Fig. 8 illustrates nicely how the bump in $M_{\eta_{NS}}$ starts growing but then fails to develop since now $\chi(T)$ melts too fast at $T_\chi/T_{\rm Ch} = 0.836$, in contrast to the mass bump in Fig. 5. That bump, namely, the strong enhancement of the η' thermal mass, is now for both susceptibilities, i.e., in both Figs. 8 and 9, encountered in their third diagrams, where $T_\chi/T_{\rm Ch} = 1$. For the four-flavor QCD, with its faster-melting $\chi(T)$, the enhancement is only some 60%, but for the SU(3) quenched QCD [with an intermediate rate of the $\chi(T)$ melting], the enhancement is drastic so that $M_{\eta'}$ and $M_{\eta_{NS}}$ mass bumps exceed the displayed scale of the figure, the maximum being roughly $M_{\eta'} \approx 2.8$ GeV. For the four-flavor QCD, such a mass bump happens in the last, "highest-$T_\chi/T_{\rm Ch}$" diagram of Fig. 9. The last diagram in the SU(3) quenched case, Fig. 8, of course exhibits even stronger $M_{\eta'}$ enhancement, although weaker than in Figs. 6 and 7 in the pure Yang-Mills case.

In summary, we tested the sensitivity of our results on variations of topological susceptibility, and found that they are sensitive to the detailed temperature behavior of $\chi(T)$. The changes are readily understood as the consequences of

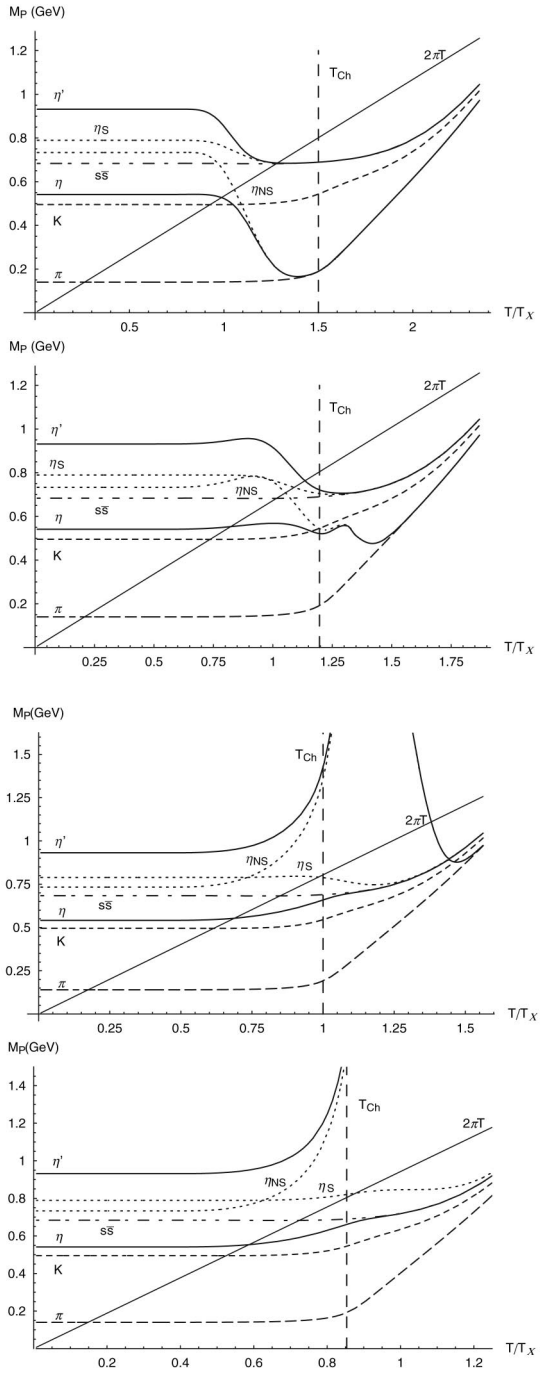

FIG. 8. The relative-temperature dependence, on T/T_χ, of the pseudoscalar meson masses for the SU(3) quenched topological susceptibility from the lattice [52]. From top to bottom, the diagrams correspond to $T_\chi = 0.667T_{\rm Ch}$, $T_\chi = 0.836T_{\rm Ch}$, $T_\chi = T_{\rm Ch}$, and $T_\chi = 1.17T_{\rm Ch}$. That means the diagrams in this composite figure correspond to the individual Figs. 1, 5, 6, and 7 (employing the pure Yang-Mills topological susceptibility). The description of the curves and symbols is the same as in these figures. In the third and fourth diagrams, $M_{\eta'}$ exceeds the scale, and the respective maxima are roughly 2.8 GeV and 7.7 GeV. What looks like a crossing of M_η and $M_{\eta'}$ in the third diagram is really a very close anticrossing, as clearly seen in the third diagram of Fig. 9.

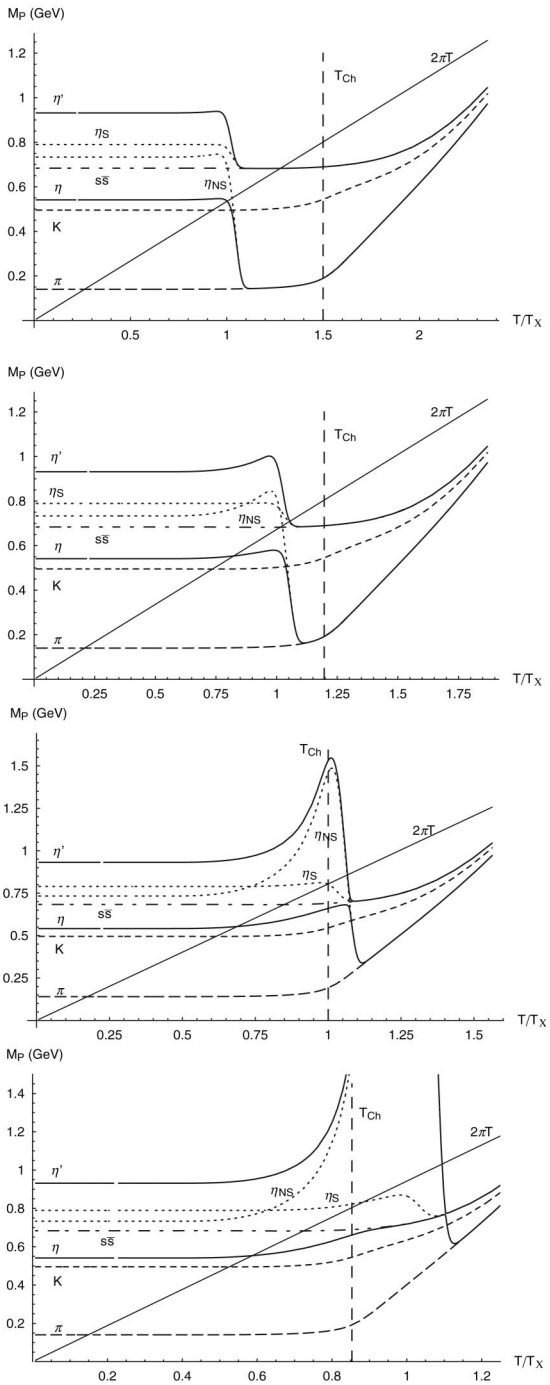

FIG. 9. The relative-temperature dependence, on T/T_χ, of the pseudoscalar meson masses. The masses in the η-η' complex are calculated employing the topological susceptibility for the four-flavor QCD taken from the lattice. From top to bottom, the diagrams correspond to $T_\chi = 0.667T_{\rm Ch}$, $T_\chi = 0.836T_{\rm Ch}$, $T_\chi = T_{\rm Ch}$, and $T_\chi = 1.17T_{\rm Ch}$. That is, the diagrams in this composite figure correspond to the parallel diagrams in the previous figure [obtained with the SU(3) quenched $\chi(T)$], as well as to the respective individual Figs. 1, 5, 6, and 7 (obtained with the pure Yang-Mills topological susceptibility). The description of the curves and symbols is the same as in these figures. In the fourth diagram, $M_{\eta'}$ exceeds the scale, and its maximum is 6.4 GeV.

the faster-melting χ's. The relative-temperature behaviors of the η mass, both in this and the previous subsection, are consistent with the $M_\eta(T)$ behaviors recently found in the NJL model by Costa *et al.* [63] for various melting rates of χ. The enhancement of the η' mass remained the most conspicuous feature for the realistic cases $T_\chi \geq T_{\rm Ch}$, but it was reduced somewhat by the faster-melting susceptibilities. Although most often still suspiciously large, the $M_{\eta'}(T)$ enhancement looks reasonable for the case of the four-flavor QCD with $T_\chi = T_{\rm Ch}$ (the third diagram in Fig. 9), where one should keep in mind that it would be further reduced in Shore's generalization.

VI. SUMMARY AND CONCLUSIONS

The separable model of Ref. [32] provides a good description of the nonstrange light mesons at $T = 0$ and $T > 0$. We extended it to the strange sector: the kaon phenomenology was successfully obtained, along with the results on the fictitious $s\bar{s}$ pseudoscalar meson, needed for the subsequent calculations of the η-η' complex. The η-η' phenomenology at $T = 0$ was then also successfully reproduced, now in this specific dynamical model [32], by following Refs. [28–31]. Thereby the stage was set for the $T > 0$ extension of the DS approach to η and η' [28–31], which is the main goal of the present paper.

The WV relation (25) enables the DS approach [28–31] to determine the masses in the η-η' complex in a parameter-free way, from the calculated nonanomalous pseudoscalar $q\bar{q}$ masses, the calculated pion decay constant f_π (resulting from our $q\bar{q}$ bound-state solutions), and the lattice results on the topological susceptibility χ, be it at $T = 0$ or $T > 0$.

The results for the thermal evolution of the masses in the η-η' complex thus depend on the choice of the topological susceptibility $\chi(T)$; in addition, the results depend even more on the relation between the chiral restoration temperature $T_{\rm Ch}$ and T_χ, the temperature of melting of the topological susceptibility. Let us recall the oldest considered scenario, namely, the Pisarski-Wilczek one, where the expected drop of the η and η' masses as $\chi(T)$ drops with T led to the expectations of the enhancement of η and η' multiplicities with growing T [26,27]. The (relative) T dependences of the masses consistent with this scenario are realized in Fig. 1, the first diagram of Fig. 8, and the first two diagrams of Fig. 9. However, this requires a rather low T_χ, noticeably below $T_{\rm Ch}$. This is unrealistic, as the values of T_χ lower than $T_{\rm Ch}$ are excluded by the lattice; e.g., Alles *et al.* have (in their notation, $T_\chi \to T_c$) $T_\chi \approx$ 260 MeV [52,64]. They identify this T_χ with $T_{\rm Ch}$, but for the value appropriate to the pure Yang-Mills case, which is higher than $T_{\rm Ch}$ in the presence of quarks. Also, there are the analogous, newer lattice results [53], with even higher $T_\chi \approx 300$ MeV. In both cases, T_χ is the melting temperature of the topological susceptibility of the *pure gauge*, Yang-Mills theory. It is thus natural that it is above the characteristic temperatures of the *full* QCD, which are lowered (with respect to Yang-Mills) by the presence of the quark degrees of freedom. This may cause (in analogy with $T_{\rm Ch}$) that, from the high values characterizing the pure Yang-Mills case, the physically relevant T_χ (e.g., T_χ appropriate to the full QCD topological charge parameter) gets lowered to $T_c \approx T_{\rm Ch}$ of the full QCD—but *not* to still lower values ($T_\chi < T_{\rm Ch}$) generally required to realize the Pisarski-Wilczek scenario in our model. Thus, our model indicates that this scenario and the hot QCD matter signal (increased η and η' multiplicity) associated with it [26,27] are excluded—apart from a possible partial exception, the third diagram in Fig. 9. This is the only $T_\chi \geq T_{\rm Ch}$ case where we observe that $M_\eta(T)$ suffers a significant fall. After $T = 1.1T_{\rm Ch}$, it drops to roughly half of its $T = 0$ value, i.e., to $M_\pi(T)$ which is not yet excessively thermally enhanced. Being preceded by a (modest) rise, this fall of $M_\eta(T)$ may not be able to provide an easily detectable increase of the η production, but this is the closest our DS approach gets to the Pisarski-Wilczek scenario for an acceptable value of $T_\chi/T_{\rm Ch}$.

Having mentioned the full QCD topological charge parameter appearing in Shore's generalization of the WV relation, let us add that the present paper and issues arisen therein obviously provide additional motivation for lattice calculations to determine this quantity and its melting temperature T_χ. We expect that this T_χ may turn out to be equal or close to the other characteristic temperatures of the full QCD, in analogy with the result $T_c \approx T_{\rm Ch}$; e.g., see Refs. [23–25].

This lowering of T_χ to $T_{\rm Ch}$ would help control the η' mass enhancements appearing for $T_\chi \gtrsim T_{\rm Ch}$, which become more and more dramatic as $T_\chi/T_{\rm Ch}$ grows. Except in the third diagram of Fig. 9, these enhancements are so drastic that they must, to a large extent, be an artifact of our approximations and assumptions, and one cannot rely on them quantitatively. On the other hand, their persistent appearances are at least a qualitative indication that probably $M_{\eta'}(T \gtrsim T_{\rm Ch}) > M_{\eta'}(0)$ in some T interval around $T_{\rm Ch}$. Thus, even though we cannot make quantitative predictions, on the basis of our results we expect a suppression of the η' yield after the onset of the chiral symmetry restoration in the hot QCD medium. We thus propose that the measurements of the η' multiplicity should be undertaken at RHIC and CERN LHC. Even if the η' suppression would not be seen, it would still be an interesting result because it would falsify the $T > 0$ extension of the so-far successful bound-state approach to η and η' [28–31].

In contrast to η', the mass of η does not exhibit a marked rise in any figure (except the gradual approach to the limit of the two lowest Matsubara frequencies). In fact, beyond the chiral restoration temperature, it rises somewhat more slowly than the pion mass. On the basis of these masses,

one cannot expect any suppression of the relative η/π^0 multiplicity. This is in agreement with the recent experimental results of the PHENIX Collaboration, which recently found a common suppression pattern of η and π^0 mesons at high transverse momentum in Au + Au collisions [65].

ACKNOWLEDGMENTS

We thank D. Blaschke and Yu. L. Kalinovsky for useful discussions. A. E. R. acknowledges support by RFBR Grant No. 05-02-16699, the Heisenberg-Landau program, and the HISS Dubna program of the Helmholtz Association. D. H. and D. K. were supported by MZT Project No. 119-0982930-1016. D. K. acknowledges the hospitality of Abdus Salam ICTP at Trieste.

[1] B. Muller and J. L. Nagle, Annu. Rev. Nucl. Part. Sci. **56**, 93 (2006).
[2] J. Adams *et al.* (STAR), Nucl. Phys. **A757**, 102 (2005).
[3] Light hadronic excitations above the critical temperature were conjectured and investigated already two decades ago—e.g., see Refs. [4,5], and more recently, Ref. [6].
[4] T. Hatsuda and T. Kunihiro, Phys. Rev. Lett. **55**, 158 (1985).
[5] C. DeTar, Phys. Rev. D **32**, 276 (1985).
[6] T. Hatsuda and T. Kunihiro, Phys. Rep. **247**, 221 (1994).
[7] F. Karsch, E. Laermann, and A. Peikert, Phys. Lett. B **478**, 447 (2000).
[8] F. Karsch, K. Redlich, and A. Tawfik, Eur. Phys. J. C **29**, 549 (2003).
[9] E. V. Shuryak and I. Zahed, Phys. Rev. D **70**, 054507 (2004).
[10] M. A. Stephanov, Proc. Sci. LAT2006 (2006) 024 [arXiv:hep-lat/0701002].
[11] D. B. Blaschke and K. A. Bugaev, Fiz. B **13**, 491 (2004).
[12] M. Asakawa, Y. Nakahara, and T. Hatsuda, Nucl. Phys. B, Proc. Suppl. **86**, 191 (2000).
[13] S. Datta, F. Karsch, P. Petreczky, and I. Wetzorke, Nucl. Phys. B, Proc. Suppl. **119**, 487 (2003).
[14] M. Asakawa and T. Hatsuda, Phys. Rev. Lett. **92**, 012001 (2004).
[15] E. Shuryak, Nucl. Phys. **A774**, 387 (2006).
[16] F. Karsch *et al.*, Nucl. Phys. **A715**, 701 (2003).
[17] M. Mannarelli and R. Rapp, Phys. Rev. C **72**, 064905 (2005).
[18] C. D. Roberts and S. M. Schmidt, Prog. Part. Nucl. Phys. **45**, S1 (2000).
[19] R. Alkofer and L. von Smekal, Phys. Rep. **353**, 281 (2001).
[20] A. Holl, C. D. Roberts, and S. V. Wright, arXiv:nucl-th/0601071.
[21] C. S. Fischer, J. Phys. G **32**, R253 (2006).
[22] A. Bender, D. Blaschke, Y. Kalinovsky, and C. D. Roberts, Phys. Rev. Lett. **77**, 3724 (1996).
[23] F. Karsch, Lect. Notes Phys. **583**, 209 (2002).
[24] C. Gattringer, P. E. L. Rakow, A. Schafer, and W. Soldner, Phys. Rev. D **66**, 054502 (2002).
[25] Y. Hatta and K. Fukushima, Phys. Rev. D **69**, 097502 (2004).
[26] J. I. Kapusta, D. Kharzeev, and L. D. McLerran, Phys. Rev. D **53**, 5028 (1996).
[27] Z. Huang and X.-N. Wang, Phys. Rev. D **53**, 5034 (1996).
[28] D. Klabučar and D. Kekez, Phys. Rev. D **58**, 096003 (1998).
[29] D. Kekez, D. Klabučar, and M. D. Scadron, J. Phys. G **26**, 1335 (2000).
[30] D. Kekez and D. Klabučar, Phys. Rev. D **65**, 057901 (2002).
[31] D. Kekez and D. Klabučar, Phys. Rev. D **73**, 036002 (2006).
[32] D. Blaschke, G. Burau, Y. L. Kalinovsky, P. Maris, and P. C. Tandy, Int. J. Mod. Phys. A **16**, 2267 (2001).
[33] D. Blaschke, Y. L. Kalinovsky, A. E. Radzhabov, and M. K. Volkov, Phys. Part. Nucl. Lett. **3**, 327 (2006).
[34] D. Horvatić, D. Blaschke, D. Klabučar, and A. E. Radzhabov, arXiv:hep-ph/0703115.
[35] D. Blaschke, D. Horvatić, D. Klabučar, and A. E. Radzhabov, arXiv:hep-ph/0703188.
[36] C. J. Burden, L. Qian, C. D. Roberts, P. C. Tandy, and M. J. Thomson, Phys. Rev. C **55**, 2649 (1997).
[37] R. Williams, C. S. Fischer, and M. R. Pennington, Phys. Lett. B **645**, 167 (2007).
[38] V. Bernard and U.-G. Meissner, arXiv:hep-ph/0611231.
[39] P. Maris, C. D. Roberts, S. M. Schmidt, and P. C. Tandy, Phys. Rev. C **63**, 025202 (2001).
[40] P. Petreczky, arXiv:nucl-th/0606013.
[41] D. Blaschke, M. Buballa, A. E. Radzhabov, and M. K. Volkov, arXiv:0705.0384.
[42] D. Horvatić *et al.* (work in progress).
[43] T. Feldmann, Int. J. Mod. Phys. A **15**, 159 (2000).
[44] T. Feldmann and P. Kroll, Phys. Scr. **T99**, 13 (2002).
[45] D. Kharzeev, R. D. Pisarski, and M. H. G. Tytgat, Phys. Rev. Lett. **81**, 512 (1998).
[46] D. E. Kharzeev, R. D. Pisarski, and M. H. G. Tytgat, arXiv:hep-ph/0012012.
[47] E. Witten, Nucl. Phys. **B156**, 269 (1979).
[48] G. Veneziano, Nucl. Phys. **B159**, 213 (1979).
[49] B. Lucini, M. Teper, and U. Wenger, Nucl. Phys. **B715**, 461 (2005).
[50] L. Del Debbio, L. Giusti, and C. Pica, Phys. Rev. Lett. **94**, 032003 (2005).
[51] B. Alles, M. D'Elia, and A. Di Giacomo, Phys. Rev. D **71**, 034503 (2005).
[52] B. Alles, M. D'Elia, and A. Di Giacomo, Nucl. Phys. **B494**, 281 (1997).
[53] C. Gattringer, R. Hoffmann, and S. Schaefer, Phys. Lett. B **535**, 358 (2002).
[54] R. D. Pisarski and F. Wilczek, Phys. Rev. D **29**, 338

(1984).
[55] R. D. Pisarski and L. G. Yaffe, Phys. Lett. **97B**, 110 (1980).
[56] E. V. Shuryak, Comments Nucl. Part. Phys. **21**, 235 (1994).
[57] J. B. Kogut, J. F. Lagae, and D. K. Sinclair, Phys. Rev. D **58**, 054504 (1998).
[58] J. Schaffner-Bielich, Phys. Rev. Lett. **84**, 3261 (2000).
[59] K. Fukushima, K. Ohnishi, and K. Ohta, Phys. Rev. C **63**, 045203 (2001).
[60] H. Meyer-Ortmanns and B.-J. Schaefer, Phys. Rev. D **53**, 6586 (1996).
[61] G. M. Shore, Nucl. Phys. **B744**, 34 (2006).
[62] G. M. Shore, arXiv:hep-ph/0701171.
[63] P. Costa, M. C. Ruivo, C. A. de Sousa, and Y. L. Kalinovsky, Phys. Rev. D **71**, 116002 (2005).
[64] G. Boyd *et al.*, Nucl. Phys. **B469**, 419 (1996).
[65] S. S. Adler *et al.* (PHENIX), Phys. Rev. Lett. **96**, 202301 (2006).